SEMARAK ILMU PUBLISHING

Journal of Advanced Research in Fluid Mechanics and Thermal Sciences

Journal homepage:
https://semarakilmu.com.my/journals/index.php/fluid_mechanics_thermal_sciences/index
ISSN: 2289-7879

A Well-Founded Analytical Technique to Solve 2D Viscous Flow Between Slowly Expanding or Contracting Walls with Weak Permeability

Yasir Ahmed Abdulameer[1,*], Abdul-Sattar Jaber Ali Al-Saif[1]

[1] Department of Mathematics, College of Education for Pure Science, Basrah University, Basrah, Iraq

ARTICLE INFO

Article history:
Received 25 March 2022
Received in revised form 31 May 2022
Accepted 11 June 2022
Available online 5 July 2022

Keywords:
Fourier transform; homotopy perturbation method; 2D viscous flow; convergence analysis

ABSTRACT

In this article, an analytical technique has been proposed for solving the model of two-dimensional viscous flow between slowly expanding or contracting walls with weak permeability. The idea of combining the Fourier transform and the homotopy perturbation method to yield a new technique was successful. The tables and graphs of the results of new analytical approximate solutions have illustrated the importance, usefulness, and necessity of using the new method. The results obtained showed the accuracy and efficiency of the new method compared to the previous methods, which were used to find the analytical approximate solutions for the current problem.

1. Introduction

The study of viscous flow theory, especially the flow of Newtonian and non-Newtonian fluids, has attracted the eye of scientists and engineers because of its important applications in various branches of science and technology. Many of these applications are based on non-linear ordinary or partial differential equations [8-10,17,18,22,24,25]. In the last years, several powerful methods have been developed to construct approximate solution of non-linear differential equations [1-7,19]. One of the foremost important problems of the fluid flow and which has interested many researchers that is the laminar flow of viscous fluid through a porous channel with contracting or expanding permeable walls. The seek for theoretical solutions about static flow of this kind began, as Berman [11] was able for the first time to find a series solution for the two-dimensional streamline flow of a viscous incompressible fluid during a parallel walled channel for the case of a very low cross-flow Reynolds number. This study paved the way for several researchers and authors who have studied this problem by watching the various variations of this problem, for instance, Ganji *et al.,* [13] used the homotopy perturbation method (HPM) to debate two-dimensional viscous fluid flow problem between slowly expanding or contracting walls. The comparison between the results of numerical method (NM) and the results of the homotopy perturbation method clarified that this method is very

* *Corresponding author.*
E-mail address: pepg.yasir.ahmed@uobasrah.edu.iq

https://doi.org/10.37934/arfmts.97.2.3956

effective and straight-forward and might be applied for other nonlinear problems. Rahimi *et al.,* [23] applied the homotopy analysis method (HAM) and homotopy perturbation method (HPM) to review of two-dimensional viscous flow between slowly expanding or contracting walls with weak permeability. The results from the two methods are compared with numerical solution by fourth order Runge–Kutta–Fehlberg technique. Furthermore, the results of dimensionless parameters on the velocity distributions are investigated. Dinarvand [12] studied the viscous fluid flow through slowly expanding or contracting walls by using the differential transform method (DTM). The comparison between the simulation results using DTM with the simulation results using the shooting method coupled with 4th-order Runge-Kutta showed remarkable accuracy. Moreover, he noticed that the differential transformation method can be used to solve many nonlinear differential equations and integral equations. Sobamowo [26] discussed two-dimensional flow of viscous fluid in an exceedingly porous channel through slowly expanding or contracting walls with injection or suction by using variation parameter method (VPM). From this study it was found that an increase in the Reynolds number of the flow process leads to a decrease in the axial velocity in the center of the channel during expansion. In addition, the axial velocity increases slightly near the surface of the channel when the wall contracts at the identical rate. Also, because the wall expansion ratio increases, the rate at the center decreases, but it increases near the wall. Sushila *et al.,* [27] applied the Sumudu transform homotopy perturbation method (HPSTM) to unravel the matter of two-dimensional viscous flow between slowly expanding or contracting walls with weak permeability. The numerical solutions showed that the proposed method is incredibly efficient and computationally attractive. Al-Saif and Al-Griffi [5] introduced a brand of a new technique to resolve two-dimensional viscous fluid flow among slowly expanding or contracting walls. This technique depends on combining the algorithms of Yang transform and the homotopy perturbation method. The results, obtained from the first iteration, showed the accuracy and efficiency of this method.

Despite the improvements of some methods that researchers used during previous studies to solve nonlinear flow problems, some of these methods require large time and effort in order to get a solution for these problems, especially the HPM [14-16] and the VPM [26] to solve the current problem. In addition to what was mentioned, many integral transformations (Fourier transform, Laplace transform, ...), are sometimes difficult to use to find exact solutions to some non-linear problems. These reasons prompted us to propose a new technique through which we seek to overcome some of the difficulties mentioned in the methods used to find a solution to such problems. Relying on previous studies and through our modest information, it was found that combining integrative transformations and analytical approximate methods may reduce many defects and difficulties facing each method individually. Therefore, we proposed merging Fourier transform (FT) with the homotopy perturbation method (HPM) to obtain a hybrid procedure that we will symbolize (FT-HPM). In addition to that, we did not find an application for this technique on non-linear flow problems, especially for the current problem in the previous literature. The most important characteristics of this method is to reduce the computations related to the integrative operations when using the homotopy perturbation method individually. Moreover, the property of convolution theory can be applied in the new method in order to reduce the difficulty of using Fourier transform in solving nonlinear differential equations. In this paper, the hybrid FT-HPM is used to find analytical approximate solutions to the problem of the two-dimensional flow of viscous fluid between slowly expanding or contracting walls. The new approximate solutions obtained using the proposed new method to address the current problem reflect the efficiency and high accuracy to FT-HPM, in addition, the analysis of solutions convergence was studied through a theorem-proof and the conclusion of the necessary convergence condition of these solutions. The tabular and graphical results and compared to the results available in previous works are showing the importance, usefulness, and necessity of using the proposed new method with reasonable convergence and accuracy. The research is organized as the following. In section 2, the basic idea of the HPM is presented. In section 3, we show the main algorithm which is characterized by extending the homotopy perturbation method using Fourier transform. Sections 4 and 5 contain the governing mathematical equations and applying the new method to the mathematical model respectively. Section 6 contains results and discussion. In section 7, convergence analysis of the proposed method is studied. Finally, the conclusions are summarized.

2. Basic Idea of Homotopy Perturbation Method

The homotopy perturbation method (HPM) was established by He J. Huan in 1998 [15,16]. This method is a powerful and efficient technique for solving differential and integral equations, linear and nonlinear. This method has a great advantage because it provides an approximate solution to a wide variety of nonlinear problems in applied science. In this method the solution is considered as the summation of an infinite series, [14]. To explain the idea of this method, let us consider the following non-linear differential equation:

$$A(u) - q(x) = 0, x \in \Omega, \tag{1a}$$

subject to the boundary conditions

$$B(u, \frac{\partial u}{\partial n}) = 0, x \in \Gamma, \tag{1b}$$

where A represent a general differential operator, u is the unknown function, $q(x)$ is a known analytic function, B is a boundary operator, and Γ is the boundary of the domain Ω. The operator A can be generally decomposed into two operators, L and N, where L is a linear operator and N is a nonlinear operator. Moreover, Eq. (1a) can be rewritten as follows:

$$L(u) + N(u) - q(x) = 0. \tag{1c}$$

By using the homotopy perturbation technique, we construct a homotopy $U(x,p): \Omega \times [0,1] \longrightarrow \mathbb{R}$, which satisfies

$$H(U,p) = (1-p)[L(U) - L(u_0)] + p[A(U) - q(x)] = 0, \tag{2a}$$

Or

$$H(U,p) = L(U) - L(u_0) + pL(u_0) + p[N(U) - q(x)] = 0, \tag{2b}$$

where $p \in [0,1]$ is an impeding parameter and u_0 is an initial approximation for the solution of Eq. (1a), which satisfies the boundary conditions. Obviously, from Eq. (2a) or Eq. (2b), we will have

$$\begin{aligned} H(U,0) &= L(U) - L(u_0) = 0, \\ H(U,1) &= A(U) - q(x) = 0. \end{aligned} \tag{3}$$

Therefore, the solution of Eq. (2a) or Eq. (2b) can be expressed as a power series in term of p as follows:

$$U=\sum_{j=0}^{\infty} p^j U_j \tag{4}$$

Setting $p=1$, then the approximate solution of Eq. (1a) can be given by

$$u=\lim_{p\to 1} U=\sum_{j=0}^{\infty} U_j. \tag{5}$$

3. Fundamental Algorithm of FT-HPM

The main objective in this section is to develop the homotopy perturbation method using Fourier transform to obtain a new technique. To explain the fundamental algorithm of this technique, we reformulate Eq. (1a) as follows:

$$L(U)+R(U)+N(U)=q(x) \tag{6}$$

with the initial condition $U(x,0)$, where $L=\partial^n/\partial t^n$ is the linear differential operator, R is the linear differential operator of less order than L, N denotes the general nonlinear differential operator, and $q(x)$ represents the source term. Moreover, the main steps of this method can be summarized as follows. By using the HPM, we have

$$(1-p)[L(U)-L(u_0)]+p[A(U)-q(x)]=0. \tag{7}$$

Taking the Fourier transform on both sides of Eq. (7), we get

$$\mathcal{F}\big[(1-p)[L(U)-L(u_0)]+p[A(U)-q(x)]\big]=0, \tag{8}$$

where, $\mathcal{F}[g(t)]=\mathcal{F}(\omega)=\int_{-\infty}^{\infty} g(t)e^{-i\omega t}\,dt$.

Postulate that $A(U)=L(U)+R(U)+N(U)$ and $L=\frac{\partial^n}{\partial t^n}$, then, we obtain

$$\mathcal{F}\left[\frac{\partial^n}{\partial t^n}(U)\right]=\mathcal{F}[L(u_0)]-p\mathcal{F}[L(u_0)]-p\mathcal{F}[R(U)+N(U)-q(x)]. \tag{9}$$

According to the homotopy perturbation method, we assume that

$$U=\sum_{j=0}^{\infty} p^j U_j, \tag{10a}$$

and the non-linear term can be expressed as follows

$$N(U)=\sum_{j=0}^{\infty} p^j H_j. \tag{10b}$$

where $H_j(U)$ are He's polynomials [27] that are given by

$$H_j(U_0,U_1,U_2,\ldots,U_j)=\frac{1}{j!}\frac{\partial^j}{\partial p^j}\left[N\left(\sum_{i=0}^{\infty} p^i U_i\right)\right]_{p=0},\ j=0,1,2,3,\ldots \tag{11}$$

Substituting Eq. (10a) and (10b) in to Eq. (9), we get

$$\mathcal{F}\left[\frac{\partial^n}{\partial t^n}\sum_{j=0}^{\infty} p^j U_j\right] = \mathcal{F}[L(u_0)] - p\mathcal{F}[L(u_0)] - p\mathcal{F}\left[R\left(\sum_{j=0}^{\infty} p^j U_j\right) + \sum_{m=0}^{\infty} p^j H_j - q(x)\right]. \tag{12}$$

Using the differentiation property of the Fourier transform, we have

$$(i\omega)^n \mathcal{F}\left[\sum_{j=0}^{\infty} p^j U_j\right] = \mathcal{F}[L(u_0)] - p\mathcal{F}[L(u_0)] - p\mathcal{F}\left[R\left(\sum_{j=0}^{\infty} p^j U_j\right) + \sum_{m=0}^{\infty} p^j H_j - q(x)\right]. \tag{13}$$

The rearrangement of Eq. (13), leads to

$$\mathcal{F}\left[\sum_{j=0}^{\infty} p^j U_j\right] = \frac{1}{(i\omega)^n}\mathcal{F}[L(u_0)] - \frac{1}{(i\omega)^n} p\mathcal{F}\left[L(u_0) + R\left(\sum_{j=0}^{\infty} p^j U_j\right) + \sum_{m=0}^{\infty} p^j H_j - q(x)\right]. \tag{14}$$

Now applying the inverse Fourier transform on both sides of Eq. (14), we get

$$\sum_{j=0}^{\infty} p^j U_j = \mathcal{F}^{-1}\left[\frac{1}{(i\omega)^n}\mathcal{F}[L(u_0)]\right] - \mathcal{F}^{-1}\left[\frac{1}{(i\omega)^n} p\mathcal{F}\begin{bmatrix} L(u_0) + R\left(\sum_{j=0}^{\infty} p^j U_j\right) \\ + \sum_{m=0}^{\infty} p^j H_j - q(x) \end{bmatrix}\right]. \tag{15}$$

Comparing the coefficient of like powers of p, we have

$$\begin{aligned}
p^0&: U_0 = \mathcal{F}^{-1}\left[\frac{1}{(i\omega)^n}\mathcal{F}[L(u_0)]\right], \\
p^1&: U_1 = -\mathcal{F}^{-1}\left[\frac{1}{(i\omega)^n}\mathcal{F}\left[L(u_0) + R\left(U_0(x)\right) + H_0(U) - q(x)\right]\right], \\
p^2&: U_2 = -\mathcal{F}^{-1}\left[\frac{1}{(i\omega)^n}\mathcal{F}\left[R\left(U_1(x)\right) + H_1(U)\right]\right], \\
&\vdots \\
p^j&: U_j = -\mathcal{F}^{-1}\left[\frac{1}{(i\omega)^n}\mathcal{F}\left[R\left(U_{j-1}(x)\right) + H_{j-1}(U)\right]\right].
\end{aligned} \tag{16}$$

Setting $p = 1$, then the analytical approximate solution u is given by

$$u = \lim_{p\to 1} U = \sum_{j=0}^{\infty} U_j. \tag{17}$$

4. Mathematical Formulation

Consider the laminar, isothermal and incompressible flow during a rectangular domain bounded by two permeable surfaces that enable the fluid to enter or exit during successive expansions or contractions [21]. A schematic diagram of the matter is shown in Figure 1. Both walls are assumed to own equal permeability and to expand uniformly at a time dependent rate $\dot{\alpha}$. Furthermore, the origin $x^* = 0$ is assumed to be the center of the classic squeeze film problem. This allows us to assume flow symmetry about $x^* = 0$.

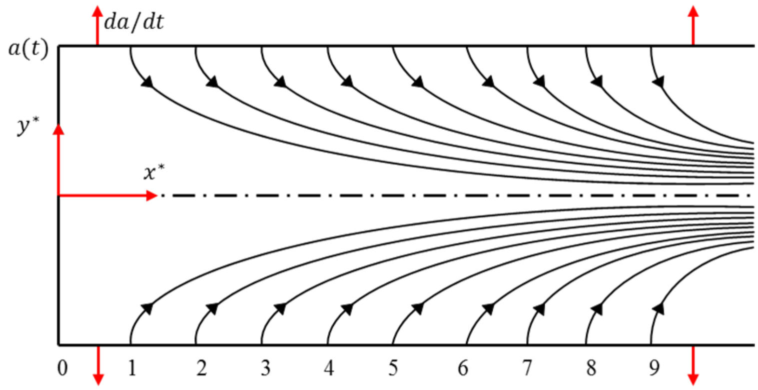

Fig. 1. Two-dimensional domain with expanding or contracting porous walls

Under the above assumptions, the equations for continuity and motion become

$$\frac{\partial U^*}{\partial x^*}+\frac{\partial V^*}{\partial y^*}=0 \tag{18}$$

$$\frac{\partial U^*}{\partial t}+U^*\frac{\partial U^*}{\partial x^*}+V^*\frac{\partial U^*}{\partial y^*}=-\frac{1}{\rho}\frac{\partial P^*}{\partial x^*}+\upsilon\nabla^2 U^* \tag{19}$$

$$\frac{\partial V^*}{\partial t}+U^*\frac{\partial V^*}{\partial x^*}+V^*\frac{\partial V^*}{\partial y^*}=-\frac{1}{\rho}\frac{\partial P^*}{\partial x^*}+\upsilon\nabla^2 V^* \tag{20}$$

where the symbols, U^* and V^* represent the components of velocity in x^* and y^* directions, P^*, ρ, υ, and t are the dimensional pressure, density, kinematic viscosity, and time**.** The boundary conditions can be specified as follows

$$y^*=a(t):\quad U^*=0, V^*=-V_w=-\dot{a}/c, \tag{21}$$

$$\begin{aligned}&y^*=0:\quad \frac{\partial U^*}{\partial y^*}(x^*,0)=0,\ V^*(x^*,0)=0,\\ &x^*=0:\quad U^*(0,y^*)=0.\end{aligned} \tag{22}$$

where, $c(c=\dot{a}/V_w)$ indicates the wall permeance or suction/injection coefficient, that is a gauge for wall permeability. The velocity components U^* and V^* can be computed from the stream function (Ψ^*) as [21]

$$U^*=\frac{\partial\Psi^*}{\partial y^*}, V^*=-\frac{\partial\Psi^*}{\partial x^*} \tag{23}$$

and mean flow vorticity (η^*) can be defined by putting [21]

$$\eta^*=\frac{\partial \mathrm{V}^*}{\partial x^*}-\frac{\partial \mathrm{U}^*}{\partial y^*}, \tag{24}$$

$$\frac{\partial\eta^*}{\partial t}+U^*\frac{\partial\eta^*}{\partial x^*}+V^*\frac{\partial\eta^*}{\partial y^*}=\upsilon\left[\frac{\partial^2\eta^*}{\partial x^{*2}}+\frac{\partial^2\eta^*}{\partial y^{*2}}\right]. \tag{25}$$

Substituting Eq. (24) into Eq. (25), we get

$$V^*{}_{x^*t} - U^*{}_{y^*t} + U^*\left(V^*{}_{x^*x^*} - U^*{}_{y^*x^*}\right) + V^*\left(V^*{}_{x^*y^*} - U^*{}_{y^*y^*}\right) = v\begin{bmatrix} V^*{}_{x^*x^*x^*} - U^*{}_{y^*x^*x^*} + \\ V^*{}_{x^*y^*y^*} - U^*{}_{y^*y^*y^*} \end{bmatrix}. \quad (26)$$

According to the mass conservation, a similar solution can be developed with respect to x^* starting with [13]

$$\Psi^* = \frac{vx^*h^*(y,t)}{a}, U^* = vx^*a^{-2}h_y^*, V^* = -va^{-1}h^*(y,t), y = \frac{y^*}{a}, h_y^* = \frac{\partial h^*}{\partial y}. \quad (27)$$

From Eq. (26) and (27), we deduce

$$U^*{}_{y^*t} + U^*U^*{}_{y^*x^*} + V^*U^*{}_{y^*y^*} = v\left[U^*{}_{y^*x^*x^*} + U^*{}_{y^*y^*y^*}\right]. \quad (28)$$

In order to solve Eq. (25), one uses the chain rule to get the following

$$h_{yyyy}^* + \alpha\left(yh_{yyy}^* + 3h_{yy}^*\right) + h^*h_{yyy}^* - h_y^*h_{yy}^* - a^2v^{-1}h_{yyt}^* \quad (29)$$

Together with the following boundary conditions

$$\begin{aligned} y = 0 &\Rightarrow h^* = 0, h_{yy}^* = 0, \\ y = 1 &\Rightarrow h^* = Re, h_y^* = 0, \end{aligned} \quad (30)$$

where $\alpha(t) = a\dot{a}/v$ denotes the non-dimensional wall dilation rate, which is positive for expansion and negative for contraction. Furthermore, $Re = aV_w/v$ refers to the Reynolds number which is positive for injection and negative for suction through the walls. Eqs. (27), (29) and (30) can be normalized as follows [20]

$$\Psi = \frac{\Psi^*}{\mathrm{a}\dot{\mathrm{a}}}, \mathrm{U} = \frac{\mathrm{U}^*}{\dot{\mathrm{a}}}, V = \frac{V^*}{\dot{a}}, h = \frac{h^*}{Re}. \quad (31)$$

Thus,

$$\Psi = \frac{xh}{c}, \mathrm{U} = \frac{\mathrm{x}h'}{\mathrm{c}}, V = \frac{-h}{c}, c = \frac{\alpha}{Re}. \quad (32)$$

Therefore, Eq. (29) becomes

$$h'''' + \alpha(yh''' + 3h'') + Re\, hh''' - Reh'h'' = 0 \quad (33)$$

with the boundary conditions

$$h(0) = 0, h''(0) = 0 \text{ and } h(1) = 1, h'(1) = 0 \quad (34)$$

where, $y = \frac{y^*}{a}$, $h = -\frac{a}{v}V^*$, $h' = \frac{d}{dy}$, $h'' = \frac{d^2}{dy^2}$, $h''' = \frac{d^3}{dy^3}$ and $h'''' = \frac{d^4}{dy^4}$. Note that Berman's [11] well-known ODE can be viewed as a special case of Eq. (33) with $\alpha = 0$.

5. Application of FT-HPM

In this section, we apply FT-HPM to get an approximate analytical solution of the Eq. (33) with the boundary conditions (34). The essential steps of this method are illustrated as follows

Applying the HPM, we have

$$h'''' - h_0'''' + ph_0'''' + p[\alpha(yh''' + 3h'') + Re\,(hh''' - h'h'') - q(y)] = 0, \tag{35}$$

Since, $h_0(y) = q(y) = 0$, then Eq. (35) become

$$h'''' = -p[\alpha(yh''' + 3h'') + Re\,(hh''' - h'h'')]. \tag{36}$$

By taking the Fourier transform on both sides of Eq. (36), we get

$$\mathcal{F}[h''''] = -p\mathcal{F}[\alpha(yh''' + 3h'') + Re\,hh''' - Reh'h''], \tag{37}$$

According to the assumption of the homotopy perturbation method, we have

$$h = \sum_{j=0}^{\infty} p^j h_j, \tag{38}$$

and the nonlinear terms can be decomposed as

$$hh''' = \sum_{j=0}^{\infty} p^j H_j \text{ and } h'h'' = \sum_{j=0}^{\infty} p^j H_j^*(y) \tag{39}$$

Substituting Eq. (38) and (39) in Eq. (37), we get

$$\mathcal{F}\left[\sum_{j=0}^{\infty} p^j h_j''''(y)\right] = -p\mathcal{F}\begin{bmatrix} Re\left(\sum_{j=0}^{\infty} p^j H_j(y) - \sum_{j=0}^{\infty} p^j H_j^*(y)\right) + \\ \alpha\left(y\sum_{j=0}^{\infty} p^j h_j'''(y) + 3\sum_{j=0}^{\infty} p^j h_j''(y)\right) \end{bmatrix}. \tag{40}$$

Comparing the coefficient of like powers of p, we get

$$p^0: \mathcal{F}[h_0''''] = 0 \Longrightarrow h_0'''' = 0, \tag{41a}$$

$$h_0(0) = 0, h_0''(0) = 0, h_0(1) = 1, h_0'(1) = 0. \tag{41b}$$

$$p^1: \mathcal{F}[h_1''''] = -\mathcal{F}[Re(H_0 - H_0^*) + \alpha(yh_0''' + 3h_0'')], \tag{42a}$$

$$h_1(0) = 0, h_1''(0) = 0, h_1(1) = 0, h_1'(1) = 0. \tag{42b}$$

$$p^2: \mathcal{F}[h_2''''] = -\mathcal{F}[Re(H_1 - H_1^*) + \alpha(yh_1''' + 3h_1'')], \tag{43a}$$

$$h_2(0) = 0, h_2''(0) = 0, h_2(1) = 0, h_2'(1) = 0. \tag{43b}$$

$$p^j: \mathcal{F}\left[h_j''''\right] = -\mathcal{F}\left[Re\left(H_{j-1} - H_{j-1}^*\right) + \alpha\left(yh_{j-1}''' + 3h_{j-1}''\right)\right], \tag{44a}$$

$h_j(0) = 0, h_j''(0) = 0, h_j(1) = 0, h_j'(1) = 0.$ (44b)

To solve Eq. (41a), we use the integration with the boundary conditions in Eq. (41b), to get

$$h_0(y) = \frac{3}{2}y - \frac{1}{2}y^3. \tag{45}$$

Eq. (42a), (43a) and (44a) represent a non homogeneous ordinary differential equations. Moreover, its general solution can be written in the following form

$$h_j(y) = h_{j_p}(y) + h_{j_c}(y), \text{ where } h_{j_c}(y) = \frac{a_j}{6}y^3 + \frac{b_j}{2}y^2 + c_j y + d_j, j \geq 1, \tag{46a}$$

Subject to the B. Cs. $h_j(0) = 0, h_j''(0) = 0, h_j(1) = 0, h_j'(1) = 0.$ (46b)

The particular solutions $h_{j_p}(y)$ can be found by applying the fundamental steps of FT-HPM as below: Using the differentiation property of the Fourier transform on Eqs. (42a), (43a) and (44a) we get

$$\mathcal{F}\left[h_{1_p}\right] = -\frac{1}{\omega^4}\mathcal{F}[Re(H_0 - H_0^*) + \alpha(yh_0''' + 3h_0'')], \tag{47}$$

$$\mathcal{F}\left[h_{2_p}\right] = -\frac{1}{\omega^4}\mathcal{F}[Re(H_1 - H_1^*) + \alpha(yh_1''' + 3h_1'')], \tag{48}$$

$$\mathcal{F}\left[h_{j_p}\right] = -\frac{1}{\omega^4}\mathcal{F}\left[Re\left(H_{j-1} - H_{j-1}^*\right) + \alpha\left(yh_{j-1}''' + 3h_{j-1}''\right)\right]. \tag{49}$$

The inverse Fourier transform on both sides of Eq. (47), (48) and (49) gives

$$h_{1_p} = -\mathcal{F}^{-1}\left[\frac{1}{\omega^4}\mathcal{F}[Re(H_0 - H_0^*) + \alpha(yh_0''' + 3h_0'')]\right], \tag{50}$$

$$h_{2_p} = -\mathcal{F}^{-1}\left[\frac{1}{\omega^4}\mathcal{F}[Re(H_1 - H_1^*) + \alpha(yh_1''' + 3h_1'')]\right], \tag{51}$$

$$h_{j_p} = -\mathcal{F}^{-1}\left[\frac{1}{\omega^4}\mathcal{F}\left[Re\left(H_{j-1} - H_{j-1}^*\right) + \alpha\left(yh_{j-1}''' + 3h_{j-1}''\right)\right]\right]. \tag{52}$$

where,

$H_0(y) = h_0 h_0'''$ and $H_0^*(y) = h_0' h_0''$,

$H_1(y) = h_0 h_1''' + h_1 h_0'''$ and $H_1^*(y) = h_0' h_1'' + h_1' h_0''$,

The simplification of Eq. (46a) leads to the following solutions

$$h_1(y) = -\frac{Re}{560}y^7 - \frac{\alpha}{20}y^5 + \frac{1}{6}\left(\frac{9}{280}Re + \frac{3}{5}\alpha\right)y^3 + \left(-\frac{1}{280}Re - \frac{1}{20}\alpha\right)y, \tag{53}$$

$$h_2(y) = \begin{bmatrix} \left(\frac{703}{2587200}Re^2 + \frac{37}{8400}\alpha Re - \frac{\alpha^2}{175}\right)y + \\ \frac{1}{6}\left(\frac{-219}{107800}Re^2 - \frac{37}{1050}\alpha Re + \frac{39}{350}\alpha^2\right)y^3 - \left(\frac{1}{50}\alpha^2 + \frac{3}{2800}\alpha Re\right)y^5 + \\ \left(\frac{1}{140}\alpha^2 + \frac{3}{1400}\alpha Re - \frac{1}{39200}Re^2\right)y^7 + \left(\frac{Re^2}{6720} + \frac{\alpha Re}{2520}\right)y^9 - \frac{Re^2}{184800}y^{11} \end{bmatrix}. \tag{54}$$

The approximate analytical solution h is given by truncated series

$$h = \lim_{N\to\infty} \sum_{j=0}^{N} h_j. \tag{55}$$

6. Results and Discussion

Figure 2 shows the effect of different values of α on $h'(y)$ at $Re = 0$. Figure 3 and 4 explain how the derivative of velocity $h'(y)$ is affected by the different values of α at $Re = -5,5$. These figures show the expanding wall ($\alpha > 0$) and contracting wall ($\alpha < 0$) for the suction case ($Re = -5$) and injection case ($Re = 5$), respectively. In addition, Figure 5 indicates the effect of different values of Re on $h'(y)$ at $\alpha = 0.5$.

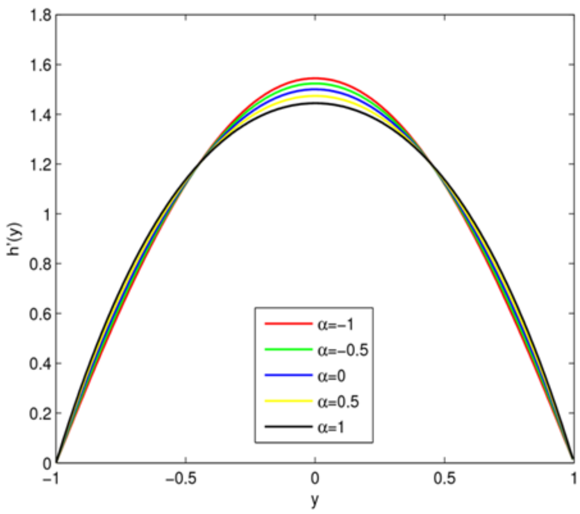

Fig. 2. The influence of various values of α on the derivative of velocity $h'(y)$ at $Re = 0$

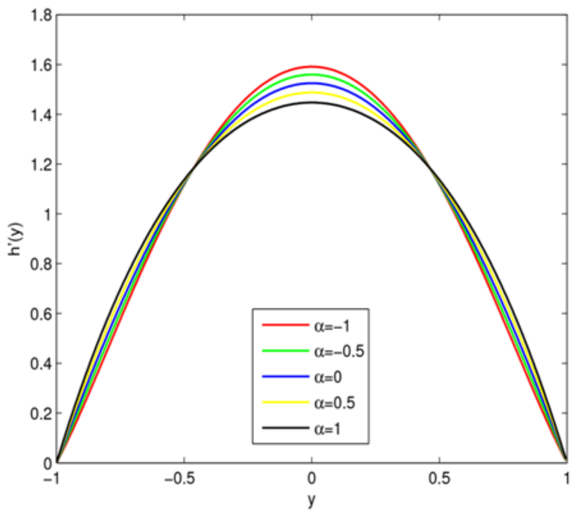

Fig. 3. The influence of various values of α on the derivative of velocity $h'(y)$ at $Re = -5$

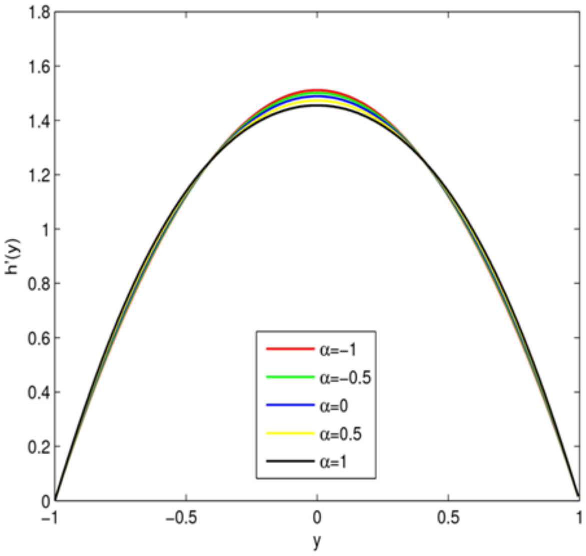

Fig. 4. The influence of various values of α on the derivative of velocity $h'(y)$ at $Re = 5$

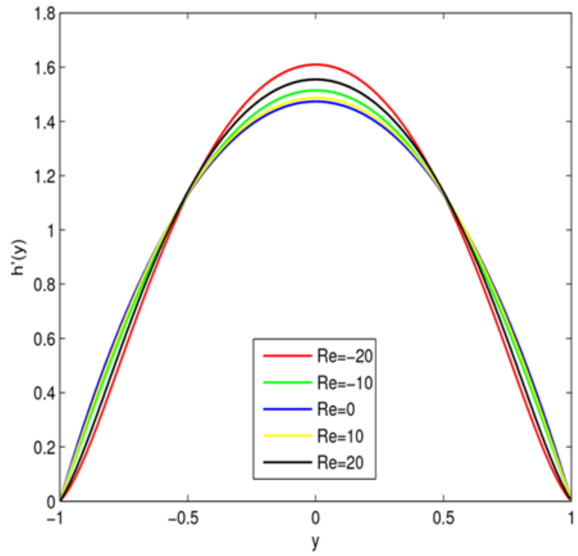

Fig. 5. The influence of various values of Re on the derivative of velocity $h'(y)$ at $\alpha\ = 0.5$

Figure 6 and Figure 7 present a comparison of the results obtained by FT-HPM, YT-HPM [5], HPM [28], VPM [26], and RK-4th of the velocity $h(y)$, when α=0.4 and $Re = 6, 10$ respectively. Figures 8 and 9 provide a comparison of the results obtained by present method (FT-HPM) and YT-HPM [5], HPM [28], VPM [26] and RK-4 of velocity $h(y)$, when choosing $Re = 4$ and α=0.1, 0.3 respectively. Figures 10 and 11 explain the comparison of the results between FT-HPM, YT-HPM [5], HPM [28], VPM [26], and RK-4th when α=0.4 and $Re = 6, 10$ for $h'(y)$, respectively.

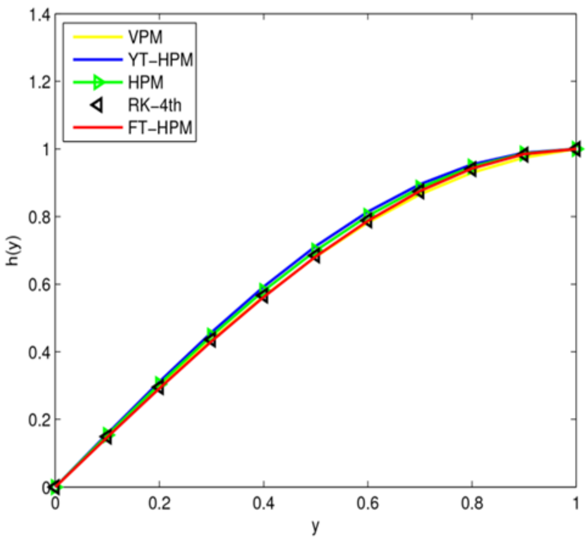

Fig. 6. Comparison of results between FT-HPM, YT-HPM [5], HPM [28], VPM [26] and RK-4th when $\alpha = 0.4$ and $Re = 6$ for $h(y)$

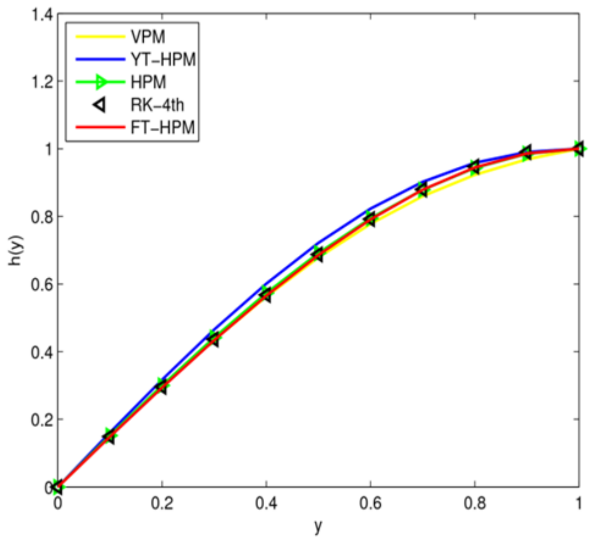

Fig. 7. Comparison of results between FT-HPM, YT-HPM [5], HPM [28], VPM [26] and RK-4th when $\alpha = 0.4$ and $Re = 10$ for $h(y)$

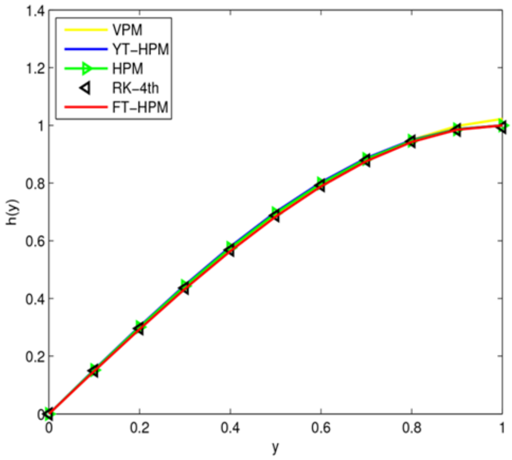

Fig. 8. Comparison of results between FT-HPM, YT-HPM [5], HPM [28], VPM [26] and RK-4th when $\alpha = 0.1$ and $Re = 4$ for $h(y)$

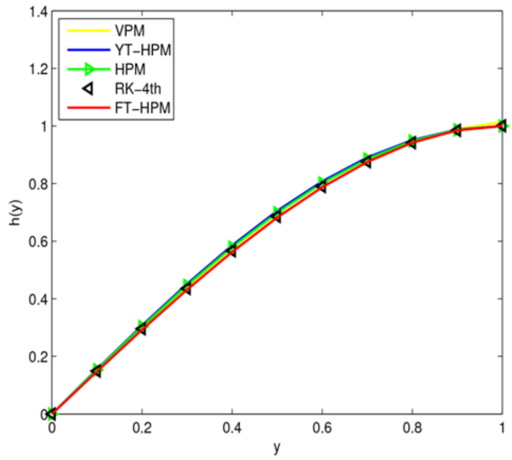

Fig. 9. Comparison of results between FT-HPM, YT-HPM [5], HPM [28], VPM [26] and RK-4th when $\alpha = 0.3$ and $Re = 4$ for $h(y)$

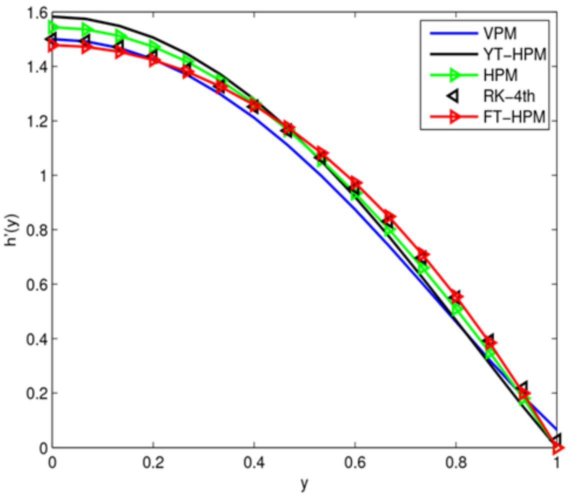

Fig. 10. Comparison of results between FT-HPM, YT-HPM [5], HPM [28], VPM [26] and RK-4th when $\alpha = 0.4$ and $Re = 6$ for $h'(y)$

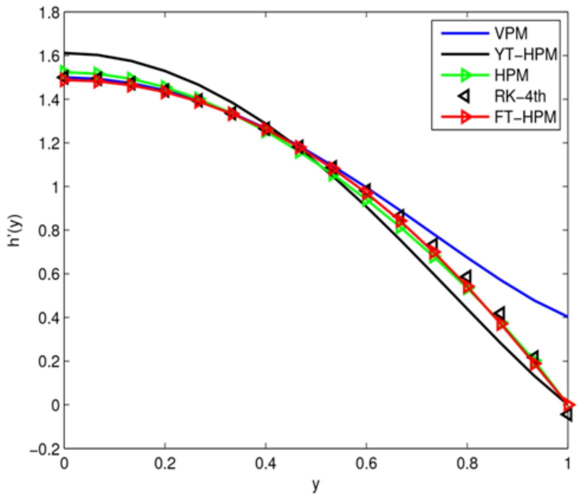

Fig. 11. Comparison of results between FT-HPM, YT-HPM [5], HPM [28], VPM [26] and RK-4th when $\alpha = 0.4$ and $Re = 10$ for $h'(y)$

In Table 1 and 2, the velocity $h(y)$ obtained by FT-HPM is compared with FY-HPM [5], HPM [28], VPM [26] and the numerical results of RK-4th when ($\alpha = 0.4$, $Re = 7$) and ($\alpha = 0.2$, $Re = 4$), respectively. The tables showed a good agreement between the analytical results of FT-HPM and numerical results of RK-4th.

Table 3 represents the comparison of the absolute errors of the approximate solutions between the two methods FT-HPM and HPM. In the upper half of the table, $Re = 5$ was chosen with different values for α ($\alpha = -0.4, 0, 0.4$), while in the lower half of the table, the comparison was made at $\alpha = 0.1$ with different values for Reynolds number ($Re = -9, 1, 9$). It is clear from this table that the absolute errors of the approximate solutions obtained using FT-HPM is less than HPM, and therefore we can say that the new method (FT-HPM) has higher accuracy and efficiency than HPM.

Table 1
Comparison of results of $h(y)$ when $\alpha = 0.4$, $Re = 7$

y	FT-HPM	YT-HPM [5]	HPM [28]	VPM [26]	RK-4th
0.0000	0.0000	0.0000	0.0000	0.0000	0.0000
0.1000	0.1475	0.1583	0.1535	0.1494	0.1495
0.2000	0.2923	0.3128	0.3034	0.2955	0.2958
0.3000	0.4316	0.4594	0.4462	0.4347	0.4359
0.4000	0.5626	0.5945	0.5787	0.5640	0.5667
0.5000	0.6824	0.7146	0.6977	0.6803	0.6854
0.6000	0.7879	0.8163	0.8002	0.7811	0.7892
0.7000	0.8758	0.8971	0.8840	0.8641	0.8755
0.8000	0.9427	0.9550	0.9466	0.9282	0.9416
0.9000	0.9852	0.9891	0.9861	0.9730	0.9844
1.0000	1.0000	1.0000	1.0000	1.0000	1.0000

Table 2
Comparison of results of $h(y)$ when $\alpha = 0.2$, $Re = 4$

y	FT-HPM	YT-HPM [5]	HPM [28]	VPM [26]	RK-4th
0.0000	0.0000	0.0000	0.0000	0.0000	0.0000
0.1000	0.1479	0.1543	0.1528	0.1495	0.1495
0.2000	0.2929	0.3051	0.3022	0.2957	0.2959
0.3000	0.4323	0.4489	0.4448	0.4356	0.4363
0.4000	0.5633	0.5824	0.5775	0.5660	0.5677
0.5000	0.6828	0.7022	0.6969	0.6840	0.6871
0.6000	0.7879	0.8052	0.8002	0.7866	0.7917
0.7000	0.8755	0.8886	0.8846	0.8714	0.8785
0.8000	0.9423	0.9500	0.9474	0.9362	0.9445
0.9000	0.9850	0.9875	0.9865	0.9794	0.9863
1.0000	1.0000	1.0000	1.0000	1.0000	1.0000

Table 3
Absolute errors comparison between FT-HPM and HPM [28] of $h(y)$

Re	α	$y = 0.1$		$y = 0.5$	
		FT-HPM	HPM [28]	FT-HPM	HPM [28]
5	-0.4	5.0060×10^{-9}	0.5865×10^{-3}	0.1916×10^{-4}	0.1856×10^{-2}
	0	6.9832×10^{-11}	0.3743×10^{-3}	0.6701×10^{-5}	0.1441×10^{-2}
	0.4	1.4221×10^{-8}	0.5049×10^{-3}	0.7515×10^{-4}	0.2362×10^{-2}
-9	0.1	4.1252×10^{-9}	0.1351×10^{-2}	0.8945×10^{-5}	0.4821×10^{-2}
1		1.5199×10^{-10}	0.4479×10^{-5}	7.3247×10^{-7}	0.2038×10^{-4}
9		7.1299×10^{-9}	0.2709×10^{-2}	0.7768×10^{-4}	0.1073×10^{-1}

After obtaining the field of the flow, the remainder of the important properties of the flow may be found. One amongst these important properties is pressure. The pressure gradient may be obtained by substituting the components of velocity into the Eq. (18)-(20). Then

$$P_y = -\left(\frac{1}{Re}h_{yy} + hh_y + \frac{\alpha}{Re}\left[h + yh_y\right]\right); P = \frac{P^*}{\rho U_W^2}. \quad (56)$$

The normal distribution of pressure can be determined by integrating Eq. (56).

The pressure distribution within the normal direction for the permeation Reynolds number $Re = \{-4, -1, 1, 4\}$ over a variety of the non-dimensional wall dilation rate α, are plotted in Figures 12-15, respectively. For each level of injection or suction shown in these figures, the pressure changes in the normal direction until it reaches a minimum near the central part.

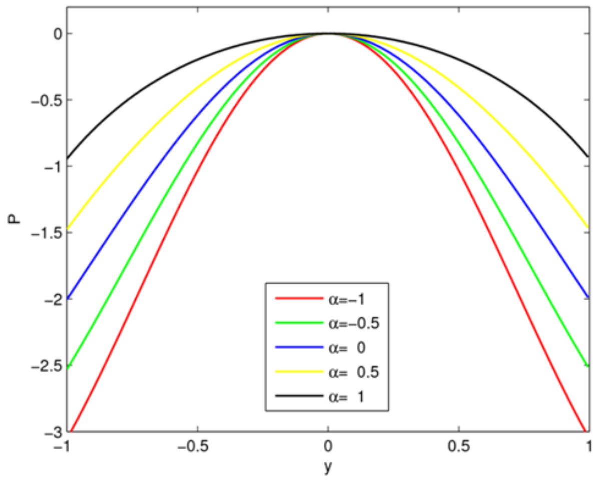

Fig. 12. The Pressure distribution over a range of α at $Re = -1$

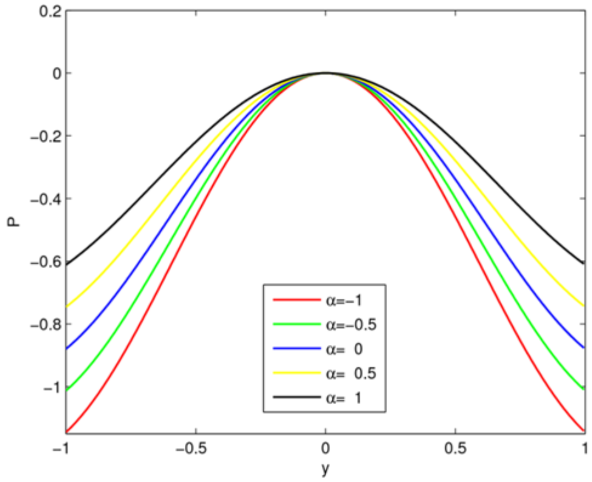

Fig. 13. The Pressure distribution over a range of α at $Re = -4$

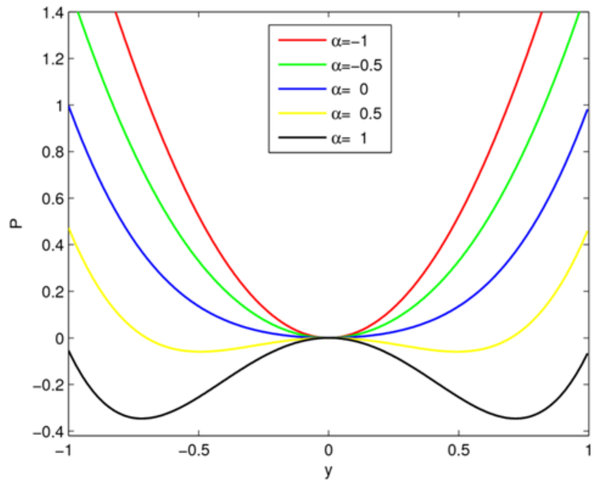

Fig. 14. The Pressure distribution over a range of α at $Re = 1$

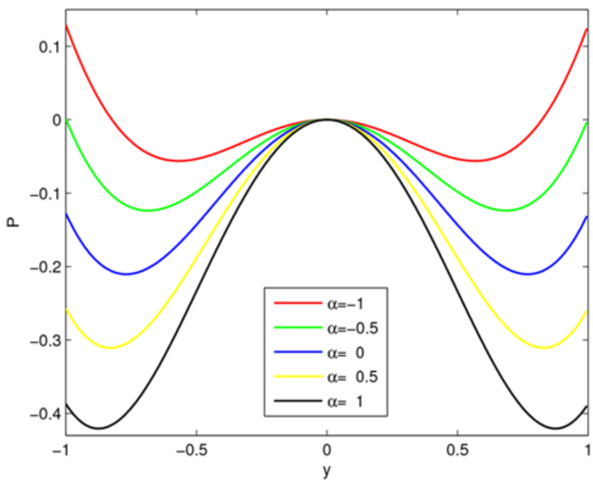

Fig. 15. The Pressure distribution over a range of α at $Re = 4$

The other property of flow is the shear stress, which can be obtained from Newton's law for viscosity in the following form

$$\tau^* = \mu\left(V^*_{x^*} + U^*_{y^*}\right) = \frac{\rho v^2 x^* h_{yy}}{a^3} \tag{57}$$

The non-dimensional shear stress is defined as: $\tau = \frac{\tau^*}{\rho V_w^2}$, then,

$$\tau = \frac{x h_{yy}(1)}{Re}. \tag{58}$$

The wall shear stress which given in Eq. (58) for the permeation Reynolds number $Re = \{-1, -4, 1\ \ 4\}$ over a spread of the non-dimensional wall dilation rate α, is plotted in Figure 16-19, respectively. It's clear from these figures that the shear stress increases along the wall surface in proportion to x^*. Thus, if α decreases, the wall shear stress increases with wall stretching ($\alpha > 0$), but increases as α increases with wall contraction ($\alpha < 0$).

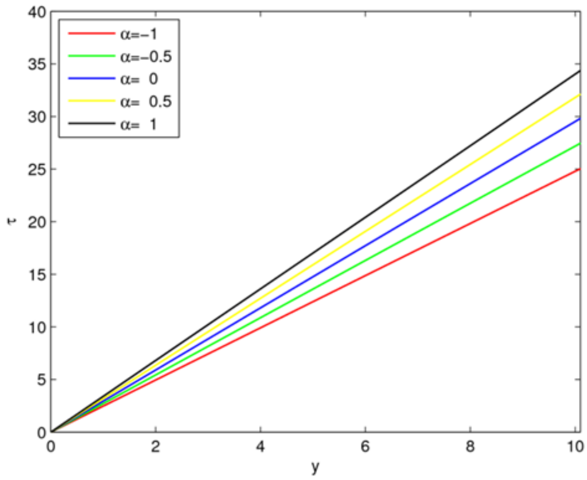

Fig. 16. The shear stress over a range of α at $Re = -1$

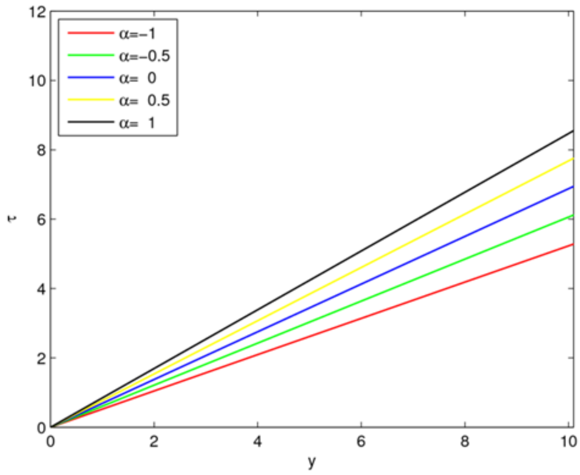

Fig. 17. The shear stress over a range of α at $Re = -4$

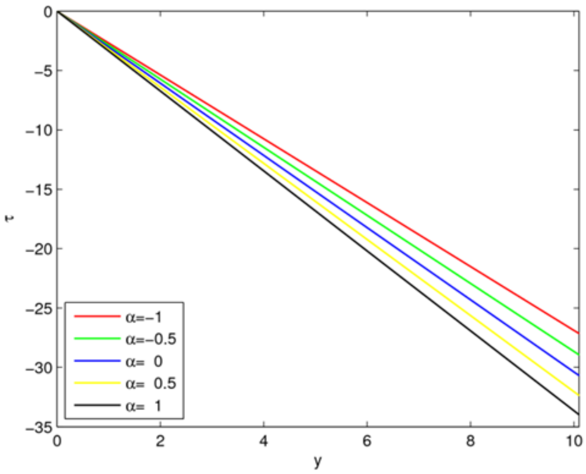

Fig. 18. The shear stress over a range of α at $Re = 1$

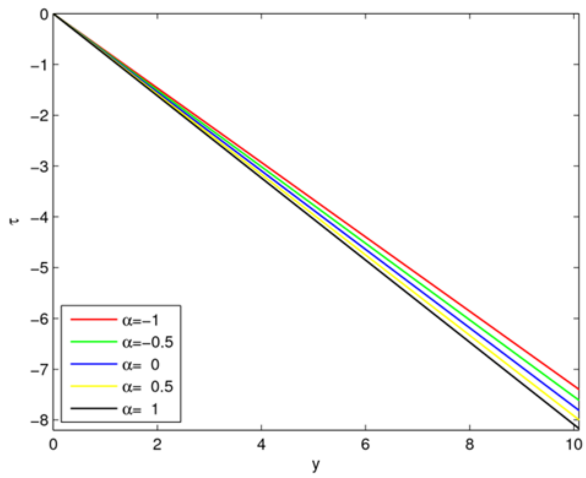

Fig. 19. The shear stress over a range of α at $Re = 4$

7. Convergence Analysis of FT-HPM

In this part, we will provide some important definitions for the study of convergence analysis with finding the necessary condition for the convergence of the approximate analytical solution (55) obtained using the approved method (FT-HPM) as follows

Definition 7.1 Suppose that $\mathcal{H}$ is the Banach space and $\mathcal{N}: \mathcal{H} \longrightarrow \mathbb{R}$ is a nonlinear mapping where $\mathbb{R}$ is the set of real numbers. Then, the sequence of the solutions can be written in the following form

$$E_{n+1} = \mathcal{N}(E_n),\ E_n = \sum_{j=0}^{n} h_j,\ j = 0,1,2,3,\ldots \tag{59}$$

where, $\mathcal{N}$ satisfies the Lipschitz condition, such that $\forall \gamma \in \mathbb{R}$,

$$\|\mathcal{N}(E_n) - \mathcal{N}(E_{n-1})\| \leq \gamma \|E_n - E_{n-1}\|,\ 0 < \gamma < 1. \tag{60}$$

Theorem 7.1 The convergence of the analytical-approximate solution $h(y) = \sum_{j=0}^{\infty} h_j(y)$ that is resulted from the application of FT-HPM converges if it satisfies the following condition

$$\|E_{n+1} - E_n\| \to 0 \text{ as } n \to \infty \text{ for } 0 < \gamma < 1. \tag{61}$$

Proof:

$$\begin{aligned}\|E_{n+1} - E_n\| &= \left\|\sum_{j=0}^{n+1} h_j - \sum_{j=0}^{n} h_j\right\| = \left\|h_0 + \sum_{j=1}^{n+1} h_j - \left[h_0 + \sum_{j=1}^{n} h_j\right]\right\| \\ &= \left\|\begin{matrix} h_0 + \sum_{j=1}^{n+1} L^{-1}\left[Re\left(H_{j-1} - H_{j-1}^*\right) + \alpha\left(yh_{j-1}''' + 3h_{j-1}''\right)\right] - \\ \left\{h_0 + \sum_{j=1}^{n} L^{-1}\left[Re\left(H_{j-1} - H_{j-1}^*\right) + \alpha\left(yh_{j-1}''' + 3h_{j-1}''\right)\right]\right\}\end{matrix}\right\| \\ &= \left\|\begin{matrix} h_0 + L^{-1}\sum_{j=1}^{n+1}\left[Re\left(H_{j-1} - H_{j-1}^*\right) + \alpha\left(yh_{j-1}''' + 3h_{j-1}''\right)\right] - \\ \left\{h_0 + L^{-1}\sum_{j=1}^{n}\left[Re\left(H_{j-1} - H_{j-1}^*\right) + \alpha\left(yh_{j-1}''' + 3h_{j-1}''\right)\right]\right\}\end{matrix}\right\|\end{aligned}$$

Since, $E_{n+1} = \mathcal{N}(E_n)$, then

$$\begin{aligned}\|E_{n+1} - E_n\| &= \left\|\begin{matrix} L^{-1}\mathcal{N}\sum_{j=0}^{n}\left[Re\left(H_{j-1} - H_{j-1}^*\right) + \alpha\left(yh_{j-1}''' + 3h_{j-1}''\right)\right] - \\ L^{-1}\mathcal{N}\sum_{j=0}^{n-1}\left[Re\left(H_{j-1} - H_{j-1}^*\right) + \alpha\left(yh_{j-1}''' + 3h_{j-1}''\right)\right]\end{matrix}\right\| \\ &= \left\| L^{-1}\mathcal{N}\left[\sum_{j=0}^{n} h_j\right] - L^{-1}N\left[\sum_{j=0}^{n-1} h_j\right] \right\| \\ &\le |L^{-1}|\left\| \mathcal{N}\left[\sum_{j=0}^{n} h_j\right] - N\left[\sum_{j=0}^{n-1} h_j\right] \right\| \\ &\le \gamma\|E_n - E_{n-1}\| = \gamma\left\|\begin{matrix}\sum_{j=0}^{n} L^{-1}\left[Re\left(H_{j-1} - H_{j-1}^*\right) + \alpha\left(yh_{j-1}''' + 3h_{j-1}''\right)\right] - \\ \left(\sum_{j=0}^{n-1} L^{-1}\left[Re\left(H_{j-1} - H_{j-1}^*\right) + \alpha\left(yh_{j-1}''' + 3h_{j-1}''\right)\right]\right)\end{matrix}\right\| \\ &\le \gamma^2\left\|\begin{matrix}\sum_{j=0}^{n-1} L^{-1}\left[Re\left(H_{j-1} - H_{j-1}^*\right) + \alpha\left(yh_{j-1}''' + 3h_{j-1}''\right)\right] - \\ \left(\sum_{j=0}^{n-2} L^{-1}\left[Re\left(H_{j-1} - H_{j-1}^*\right) + \alpha\left(yh_{j-1}''' + 3h_{j-1}''\right)\right]\right)\end{matrix}\right\| \\ &\vdots \\ &\le \gamma^n\left\|\begin{matrix}\sum_{j=0}^{1} L^{-1}\left[Re\left(H_{j-1} - H_{j-1}^*\right) + \alpha\left(yh_{j-1}''' + 3h_{j-1}''\right)\right] - \\ \left(\sum_{j=0}^{0} L^{-1}\left[Re\left(H_{j-1} - H_{j-1}^*\right) + \alpha\left(yh_{j-1}''' + 3h_{j-1}''\right)\right]\right)\end{matrix}\right\| \\ &= \gamma^n\|E_1 - E_0\| \to 0 \text{ as } n \to \infty \text{ for } 0 < \gamma < 1,\ L^{-1}(\cdot) = \mathcal{F}^{-1}\left[\frac{1}{\omega^4}\mathcal{F}(\cdot)\right]. \quad \blacksquare\end{aligned}$$

From the results of theorems 7.1, the values of the parameter γ^n can be calculated by using the following definition.

Definition 7.2 For $n = 1,2,3, \ldots$

$$\gamma^n = \begin{cases} \frac{\|E_{n+1} - E_n\|}{\|E_1 - E_0\|} = \frac{\|h_{n+1}\|}{\|h_1\|}, & \|h_1\| \ne 0, n = 1,2,3, \ldots \\ 0, & \|h_1\| = 0 \end{cases} \tag{62}$$

Definition 7.2 can be used to find the convergence of approximate solutions to the problem under study. Moreover, the results of convergence of solutions that were found were compared using the two methods FT-HPM, HPM, as shown in the following Table 4.

Table 4
Comparison of the values of the parameter γ^n between FT-HPM and HPM [28]

Re	α	Method	γ	γ^2	γ^3
1	0.5	FT-HPM	0.3778×10^{-1}	4.6039×10^{-7}	5.1247×10^{-9}
		HPM	0.3778×10^{-1}	0.6861×10^{-2}	0.8406×10^{-3}
5	0.5	FT-HPM	0.3846494238	0.4509×10^{-5}	2.3727×10^{-8}
		HPM	0.3846494239	0.7062×10^{-1}	0.2050×10^{-1}

It is clear from Table 4 that $\gamma^n \to 0$ as $n \to \infty$ for $0 < \gamma < 1$. In addition, this table shows that the powers of γ which were calculated based on FT-HPM approach to zero faster than the powers of γ calculated by HPM. Therefore, FT-HPM can be considered as a development of HPM with better convergence.

8. Conclusions

In this paper, the FT-HPM has been successfully used for solving two-dimensional viscous flow between slowly expanding or contracting walls with weak permeability. The graphical results of the present study show the influence of the non-dimensional wall dilation rate α and permeation Reynolds number Re on the velocity, normal pressure distribution and wall shear stress . Moreover, we noted that for each level of injection or suction, when the wall is expanding ($\alpha > 0$), an increase α lead up to the velocity becomes higher close to the center and lower near the wall. This happens because the flow becomes larger toward the center to compensate the area resulting from the expansion of the wall. As a result, the velocity also becomes larger close to the center. Also, for all levels of suction or injection, if the wall is contracting ($\alpha < 0$), increase α lead to the axial velocity becomes low close to the center and high near the wall, the reason that the velocity becomes larger close to the wall because the flow towards the wall becomes larger. Also, we found that this method is a powerful mathematical tool and can be applied to a large class of linear and non-linear problems with very efficiently in various fields of science and engineering, especially equations that describe fluid flow.

References

[1] Jasim, Abeer Majeed, and Abdul-Sattar JA Al-Saif. "New Travelling Wave Solutions for the Two-Dimensional Navier-Stokes and Heat Equations." (2019).

[2] Al-Muslimawi, A., H. R. Tamaddon-Jahromi, and M. F. Webster. "Simulation of viscoelastic and viscoelastoplastic die-swell flows." *Journal of Non-Newtonian Fluid Mechanics* 191 (2013): 45-56. https://doi.org/10.1016/j.jnnfm.2012.08.004

[3] Al-Muslimawi, Alaa H. "Numerical study for differential constitutive equations with polymer melts by using a hybrid finite-element/volume method." *Journal of Computational and Applied Mathematics* 308 (2016): 488-498. https://doi.org/10.1016/j.cam.2016.06.007

[4] Al-Saif, A. J. A., and Abeer Majeed Jasim. "Analytical investigation of the MHD Jeffery-Hamel flow through convergent and divergent channel by new scheme." *Engineering Letters* 27, no. 3 (2019): 646-657.

[5] Abdul-Sattar J. Al-Sai and Takia Ahmed J. Al-Griffi, "A New Technique to Solve Two-Dimensional Viscous Fluid Flow Among Slowly Expand or Contract Walls." *Mathematical Modelling of Engineering Problems* 7, no. 4 (2020).:631-641. https://doi.org/10.18280/mmep.070416

[6] Al-Saif, Abdul-Sattar J., and Assma J. Harfash. "A new approximate analytical solutions for two-and three-dimensional unsteady viscous incompressible flows by using the kinetically reduced local navier-stokes equations." *Journal of Applied Mathematics* 2019 (2019). https://doi.org/10.1155/2019/3084394

[7] Harfash, Assma Jassim, and Abdul-Sattar Jaber Al-Saif. "MHD flow of fourth grade fluid solve by perturbationiteration algorithm." *Journal of Advanced Research in Fluid Mechanics and Thermal Sciences* 59, no. 2 (2019): 220-231.

[8] Beleri, Joonabi, and Asha S. Kotnurkar. "Peristaltic Transport of Ellis Fluid under the Influence of Viscous Dissipation Through a Non-Uniform Channel by Multi-Step Differential Transformation Method." *Journal of Advanced Research in Numerical Heat Transfer* 9, no. 1 (2022): 1-18.

[9] Akaje, Wasiu, and B. I. Olajuwon. "Impacts of Nonlinear thermal radiation on a stagnation point of an aligned MHD Casson nanofluid flow with Thompson and Troian slip boundary condition." *Journal of Advanced Research in Experimental Fluid Mechanics and Heat Transfer* 6, no. 1 (2021): 1-15.

[10] Teh, Yuan Ying, and Adnan Ashgar. "Three dimensional MHD hybrid nanofluid Flow with rotating stretching/shrinking sheet and Joule heating." *CFD Letters* 13, no. 8 (2021): 1-19. https://doi.org/10.37934/cfdl.13.8.119

[11] Berman, Abraham S. "Laminar flow in channels with porous walls." *Journal of Applied physics* 24, no. 9 (1953): 1232-1235. https://doi.org/10.1063/1.1721476

[12] Saeed, Dinarv. "Reliable treatments of differential transform method for two-dimensional incompressible viscous flow through slowly expanding or contracting porous walls with small-to-moderate permeability." *International Journal of Physical Sciences* 7, no. 8 (2012): 1166-1174. https://doi.org/10.5897/IJPS11.1753

[13] Ganji, Z. Z., D. D. Ganji, and A. Janalizadeh. "Analytical solution of two-dimensional viscous flow between slowly expanding or contracting walls with weak permeability." *Mathematical and Computational Applications* 15, no. 5 (2010): 957-961. https://doi.org/10.3390/mca15050957

[14] He, Ji-Huan. "Homotopy perturbation technique." *Computer methods in applied mechanics and engineering* 178, no. 3-4 (1999): 257-262. https://doi.org/10.1016/S0045-7825(99)00018-3

[15] He, Ji-Huan. "A coupling method of a homotopy technique and a perturbation technique for non-linear problems." *International journal of non-linear mechanics* 35, no. 1 (2000): 37-43. https://doi.org/10.1016/S0020-7462(98)00085-7

[16] He, Ji-Huan. "The homotopy perturbation method for nonlinear oscillators with discontinuities." *Applied mathematics and computation* 151, no. 1 (2004): 287-292. https://doi.org/10.1016/S0096-3003(03)00341-2

[17] Fekadu, Birlie, and H. V. Harish. "Numerical Studies on Thermo-Hydraulic Characteristics of Turbulent Flow in a Tube with a Regularly Spaced Dimple on Twisted Tape." *CFD Letters* 13, no. 8 (2021): 20-31. https://doi.org/10.37934/cfdl.13.8.2031

[18] Hussin, Amil Hamja Ali, Shamsul Sarip, and Mohd Khairi Abu Husain. "Investigation of Ultrasonic-Assisted Drilling (UAD) Parameters For Hole Making Of Ti-6Al-4V Using Taguchi Method." *Journal of Advanced Research in Applied Sciences and Engineering Technology* 27, no. 1 (2022): 45-61.

[19] Fadhel, Ihssan Aqeel, and Alaa Hassan Al-Muslimawi. "Simulation of Newtonian axisymmetric pipe flow by using a Taylor Galerkin/pressure correction finite element method." *Basrah journal of science* 38, no. 2 (2020): 198-222. https://doi.org/10.29072/basjs.202024

[20] Jafaryar, M., S. Iman Pourmousavi, M. Hosseini, and E. Mohammadian. "Application of DTM for 2D viscous flow through expanding or contracting gaps with permeable walls." *New Trends in Mathematical Sciences* 2, no. 3 (2014): 145-158. https://doi.org/10.1016/j.jppr.2014.11.001

[21] Majdalani, Joseph, Chong Zhou, and Christopher A. Dawson. "Two-dimensional viscous flow between slowly expanding or contracting walls with weak permeability." *Journal of Biomechanics* 35, no. 10 (2002): 1399-1403. https://doi.org/10.1016/S0021-9290(02)00186-0

[22] Bajuri, Muhammad Nur Arham, Djamal Hissein Didane, Mahamat Issa Boukhari, and Bukhari Manshoor. "Computational Fluid Dynamics (CFD) Analysis of Different Sizes of Savonius Rotor Wind Turbine." *Journal of Advanced Research in Applied Mechanics* 94, no. 1 (2022): 7-12.

[23] Rahimi, E., A. Rahimifar, R. Mohammadyari, I. Rahimipetroudi, and M. Rahimi-Esbo. "Analytical approach for solving two-dimensional laminar viscous flow between slowly expanding and contracting walls." *Ain Shams Engineering Journal* 7, no. 4 (2016): 1089-1097. https://doi.org/10.1016/j.asej.2015.07.013

[24] Mahat, Rahimah, Muhammad Saqib, Imran Ulah, Sharidan Shafie, and Sharena Mohamad Isa. "MHD Mixed Convection of Viscoelastic Nanofluid Flow due to Constant Heat Flux." *Journal of Advanced Research in Numerical Heat Transfer* 9, no. 1 (2022): 19-25.

[25] Sharafatmandjoor, Shervin. "Effect of Imposition of viscous and thermal forces on Dynamical Features of Swimming of a Microorganism in nanofluids." *Journal of Advanced Research in Micro and Nano Engineering* 8, no. 1 (2022): 1-8.

[26] Sobamowo, Gbeminiyi Musibau. "On the analysis of laminar flow of viscous fluid through a porous channel with suction/injection at slowly expanding or contracting walls." *Journal of Computational Applied Mechanics* 48, no. 2 (2017): 319-330.

[27] Singh, Jagdev, and Y. S. Shishodia. "A reliable approach for two-dimensional viscous flow between slowly expanding or contracting walls with weak permeability using sumudu transform." *Ain Shams Engineering Journal* 5, no. 1 (2014): 237-242. https://doi.org/10.1016/j.asej.2013.07.001

[28] Ganji, Z. Z., D. D. Ganji, and A. Janalizadeh. "Analytical solution of two-dimensional viscous flow between slowly expanding or contracting walls with weak permeability." *Mathematical and Computational Applications* 15, no. 5 (2010): 957-961. https://doi.org/10.3390/mca15050957